

Alignment and pulse-duration effects in two-photon double ionization of H₂ by femtosecond XUV laser pulses

Xiaoxu Guan,^{1,*} Klaus Bartschat,¹ Barry I. Schneider,² and Lars Koesterke³

¹*Department of Physics and Astronomy, Drake University, Des Moines, Iowa 50311, USA*

²*Applied and Computational Mathematics Division, Information Technology Laboratory, National Institute of Standards and Technology, Gaithersburg, Maryland 20899, USA*

³*Texas Advanced Computer Center, University of Texas at Austin, Austin, Texas 78758, USA*

(Received 5 September 2014; published 24 October 2014)

We present calculations for the dependence of the two-photon double ionization (DI) of H₂ on the relative orientation of the linear laser polarization to the internuclear axis and the length of the pulse. We use the fixed-nuclei approximation at the equilibrium distance of $1.4 a_0$, where $a_0 = 0.529 \times 10^{-10}$ m is the Bohr radius. Central photon energies cover the entire direct DI domain from 26.5 to 34.0 eV. In contrast to the parallel geometry studied earlier [X. Guan, K. Bartschat, B. I. Schneider, and L. Koesterke, *Phys. Rev. A* **83**, 043403 (2011)], the effect of the pulse duration is almost negligible for the case when the two axes are perpendicular to each other. This is a consequence of the symmetry rules for dipole excitation in the two cases. In the parallel geometry, doubly excited states of $^1\Sigma_u^+$ symmetry affect the cross section, while in the perpendicular geometry only much longer-lived $^1\Pi_u$ states are present. This accounts for the different convergence patterns observed in the calculated cross sections as a function of the pulse length. When the photon energy approaches the threshold of sequential DI, a sharp increase of the generalized total cross section (GTCS) with increasing pulse duration is also observed in the perpendicular geometry, very similar to the case of the molecular axis being oriented along the laser polarization direction. Our results differ from those of Colgan *et al.* [J. Colgan, M. S. Pindzola, and F. Robicheaux, *J. Phys. B* **41**, 121002 (2008)] and Morales *et al.* [F. Morales, F. Martín, D. A. Horner, T. N. Rescigno, and C. W. McCurdy, *J. Phys. B* **42**, 134013 (2009)], but are in excellent agreement with the GTCSs of Simonsen *et al.* [A. S. Simonsen, S. A. Sørngård, R. Nepstad, and M. Førre, *Phys. Rev. A* **85**, 063404 (2012)] over the entire domain of direct DI.

DOI: [10.1103/PhysRevA.90.043416](https://doi.org/10.1103/PhysRevA.90.043416)

PACS number(s): 33.80.Wz, 31.15.A–

I. INTRODUCTION

Double ionization (DI) induced by photon and charged-particle impact provides a unique way to unveil the intriguing electron correlation in atoms [1–3], molecules [4–6], and surfaces [7]. With the advent of new light sources and the development of effective numerical approaches, we are now able to investigate fundamental two-electron processes on an unprecedented subfemtosecond time scale. Generally, the preferred emission direction of the second electron depends in a highly sensitive way on the direction of the first electron and also on the sharing of the available energy between the two.

In a recent paper [8], we reported potential resonance effects on theoretical predictions for two-photon DI processes in molecular hydrogen (H₂). Those calculations were performed in the fixed-nuclei approximation (FNA) at the equilibrium distance of $1.4 a_0$, with the linear laser polarization parallel to the internuclear axis. Although the nuclei are not stationary in nature, it is important to provide well-characterized benchmarks for this theoretically very challenging problem, for which vastly different predictions exist in the literature [9–11]. For the parallel geometry, we followed up on an earlier suggestion [6] that resonance effects might be responsible for these differences, in light of the fact that a number of doubly excited states with $^1\Sigma_u^+$ symmetry are located in the vicinity of 30 eV above the ground-state potential-energy curve.

An even more computationally challenging problem is presented when the polarization of the electric-field vector is perpendicular to the internuclear axis. In this instance, the azimuthal symmetry is broken and additional angular momentum states must be accounted for in the computation. For this case, too, there are major differences among theoretical predictions in the literature.

The principal goals of the present work are twofold. First, while alignment effects in the perpendicular geometry were investigated previously [6,12], these studies were limited to relatively short pulse durations and a single photon energy. Hence we considered it essential to extend the previous work by generating a set of benchmark results that can be used as a reference in future studies, where the nuclear motion should be accounted for in some way. As mentioned above, this will be necessary before a realistic comparison with any experimental data becomes possible.

Second, we address the question of whether or not doubly excited states might affect the two-photon DI of H₂ driven by a laser pulse with the polarization vector normal to the molecular axis. This study should further narrow down possible sources for the large discrepancies found in the literature, due to either the physical effects included or to numerical issues in the various treatments of the problem. For the geometry of interest here, two earlier studies [9,10] concentrated on a single photon energy (30 eV). Note that, in the present work, the terms “photon frequency” or “photon energy” ($h\nu$) for pulses always refer to the central frequency of the electric field.

As a function of photon energy, the generalized total cross sections (GTCSs) in the photon-energy regime from 26.4 to

*Current Address: Department of Physics and Astronomy, Louisiana State University, Baton Rouge, Louisiana 70803, USA.

32.7 eV were computed in the recent work by Simonsen *et al.* [11], who used B -spline bases and the FNA. In the present work, also within the framework of the FNA, we employ a full-dimensional *ab initio* approach to investigate the above problem in the photon-energy regime from 26.5 through 34.0 eV at the internuclear separation distance of $1.4 a_0$. In addition to GTCSs, we also present a variety of results for energy- and angle-resolved kinematics. While our emphasis is placed on the perpendicular geometry, some results for the parallel geometry will be presented in order to allow for a comparison between the two cases.

II. THEORETICAL AND NUMERICAL METHOD

As outlined in a number of previous papers [5,6,12], we formulate the problem in prolate spheroidal coordinates, in the fixed-nuclei approximation at the equilibrium distance of $R = 1.4 a_0$. The wave function is expanded in a finite-element discrete-variable representation (FE-DVR). The solution of the time-dependent Schrödinger equation (TDSE) is propagated in time under the influence of the laser pulse using the short iterative Lanczos method [13]. We extract generalized cross sections (GCSs) from the probability for double ionization by projecting onto two-center Coulomb functions with the appropriate energies.

The (angle- and energy-integrated) GTCS and (angle- and energy-resolved) generalized triple-differential cross section (GTDCS) are the central quantities required to study the two-photon DI of H_2 . The GCS concept has been used both theoretically [14] and experimentally [15,16] for many years to describe multiphoton ionization of atomic and molecular systems. As opposed to gas-phase collision processes induced by charged particles (electrons or protons, for example) on atomic and molecular targets, more than one incident photon can be absorbed when the target is irradiated by sufficiently intense laser fields. Formally, generalized ionization (or excitation) cross section can be introduced by the ratio of the transition rate and the incident photon flux density (Φ). This naturally yields the cross section in the units of area. However, the above definition of the cross section is not the most appropriate for N -photon processes ($N \geq 2$), since the transition rate for N -photon ionization depends on the photon flux density as Φ^N in the perturbative regime [17]. As a consequence, the conventional cross section scales as Φ^{N-1} and hence not only depends on the target but also on the external laser field. To overcome this, various (angle- and energy-integrated or -resolved) GCSs can be introduced to isolate the characteristic response of the target by dividing the transition rate by Φ^N . The resulting GTCSs are usually expressed in the dimension of $\text{cm}^{2N} \text{s}^{N-1}$, which reduces to just an area (cm^2) for one-photon processes.

Conceptually, this makes the GCSs independent of the photon flux density in the perturbative regime. It provides a practical way to examine the accuracy of numerically extracted GCSs from time-dependent calculations when the results are expected to be independent of the peak intensity as well as the temporal form of the laser pulse. To ensure the latter, it is critical to define an appropriate interaction time to account for the details of the pulse envelope [3]. Nonperturbative behavior may also be identified by deviations from the power

law for the intensity [18]. Interested readers should consult Refs. [2,3,5,12] for more details.

Rigorously, the concept of a cross section requires infinitely long “pulses” and weak intensities. In the current calculations, the peak intensity of the laser pulses is 10^{13} W/cm^2 , which is indeed weak for the extreme ultraviolet (XUV) regime. In addition, the pulses contain enough cycles for the details of the envelope function to be relatively unimportant, provided the appropriate effective interaction time is used. Therefore, it is possible to define meaningful GCSs in the parameter regime studied in this work.

Finally, projecting onto a product of Coulomb waves is valid as long as one propagates for sufficiently long times and large distances. Computationally, this can be tested by examining the predictions of the projection at different times after the laser has been switched off and monitoring the convergence of the results (see, for example, Refs. [5,19,20]). In the present study, the GCSs were generally extracted at the moment corresponding to two cycles of field-free propagation after the laser was switched off, but spot checks were performed for extraction times up to ten cycles after the pulse (see also Sec. III). The results presented below were found to be stable against reasonable variations in the numerical details, such as the number of and distribution of the DVR functions, the size of the box, the number of partial waves retained in the expansion of the wave function, and the time after the pulse at which the information is extracted.

To summarize, all our calculations employed a laser pulse with a well-defined integer number of optical cycles (o.c.). A \sin^2 envelope function was used. In contrast to a convention often favored in experiments, the pulse length is *not* defined by the full width at half maximum of the temporal intensity, but rather by the number of complete cycles with nonzero electric field. The carrier-envelope phase was set to zero.

III. RESULTS AND DISCUSSION

The angle-integrated GTCSs for DI of the H_2 molecule for various cases are displayed in Fig. 1. At $h\nu = 30 \text{ eV}$, all previously published time-dependent results [6,9,11] employed an interaction time between 1.4 and 2.1 femtoseconds (fs), i.e., 10–15 o.c. For the perpendicular geometry shown in Fig. 1(a), the dependence of our results on the pulse length is small for central photon energies up to about 33 eV, as shown by examining predictions obtained with 10, 20, and 30 o.c. When approaching the threshold for sequential DI, on the other hand, the rapid increase of the GTCS is not at all captured by the 10-o.c. pulse. Our results for 20 o.c. are in excellent agreement with the *ab initio* calculations by Simonsen *et al.* [11], which were performed using an entirely independent method, but with similar laser parameters (15 o.c. as the pulse duration). The simplified model of Ref. [11] also does reasonably well, but over most of the energy range it predicts slightly lower GTCSs than the direct solution of the TDSE. The time-dependent close-coupling (TDCC) results of Colgan *et al.* [9] and the exterior complex scaling (ECS) predictions of Morales *et al.* [10] for a photon energy of 30 eV are about a factor of 2 larger than our TDSE results at this energy.

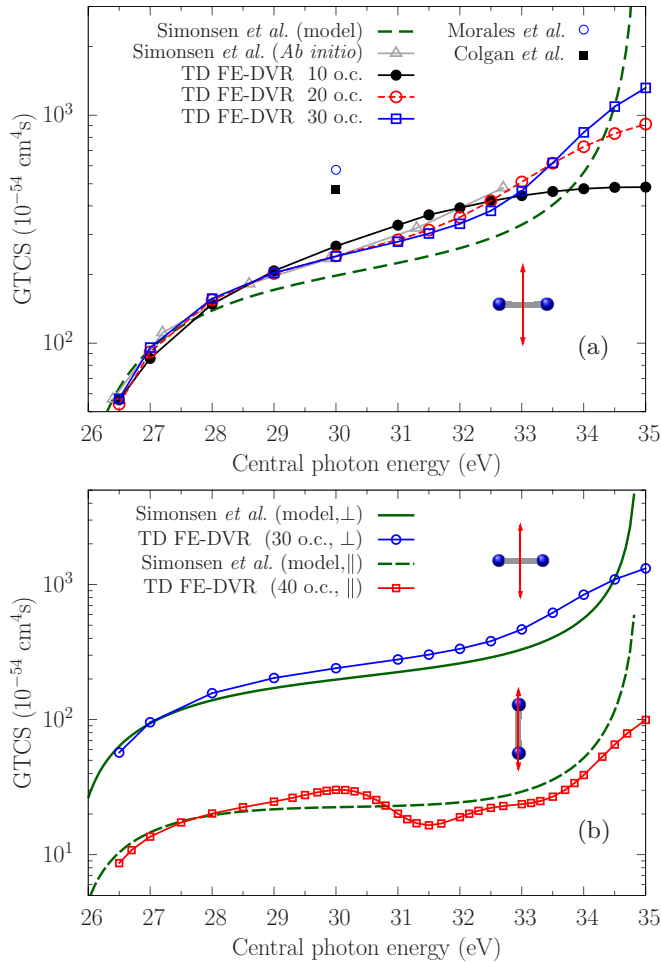


FIG. 1. (Color online) GTCS for two-photon DI of the H_2 molecule. In panel (a), the molecular axis is oriented perpendicular to the linear polarization vector (represented by a double-headed arrow) of the laser pulse. Our present results were obtained for pulse lengths of 10, 20, and 30 optical cycles. Also shown are the *ab initio* and the model results of Simonsen *et al.* [11], as well as the cross sections of Colgan *et al.* [9] and Morales *et al.* [10] at 30 eV. Panel (b) shows a comparison between our *ab initio* results obtained in the perpendicular (\perp) and parallel (\parallel) geometries, with the corresponding predictions from a simple model suggested by Simonsen *et al.* [11].

As discussed earlier in some detail [8], major discrepancies between the TDCC and ECS predictions, and subsequently with our own calculations [6], also occurred for the parallel geometry. There it was conceivable that resonance effects, which were investigated by changing the pulse length, play a role. As discussed above, however, this is an unlikely explanation for the discrepancies in the perpendicular case. There are no doubly excited states with ${}^1\Pi_u$ symmetry located in the vicinity of 30 eV for the equilibrium internuclear separation, and hence in this case the GTCS at 30-eV photon energy is well converged. As a consequence, the lack of dependence on the pulse length seen in Fig. 1(a) is understandable. In fact, our results at this photon energy are well converged with respect to the pulse length, to the value of $2.40 \times 10^{-52} \text{ cm}^4 \text{ s}$. Increasing the pulse duration from 20 cycles to 30 cycles changes the result by less than 0.5%. The total cross section

obtained in Ref. [11] is $2.349 \times 10^{-52} \text{ cm}^4 \text{ s}$ at 29.9 eV, in excellent agreement with our number. The TDCC and ECS results at 30.0 eV, on the other hand, are 4.7×10^{-52} [9] and $5.76 \times 10^{-52} \text{ cm}^4 \text{ s}$ [10], respectively.

As mentioned previously, a few words concerning the extraction of the GCSs are in order. Consider the example of a ten-cycle pulse for the parallel geometry at an energy of 30 eV. Results were obtained by propagating for two and ten cycles after the laser pulse was turned off and projecting onto a product of uncorrelated Coulomb waves. Comparing the two results revealed changes in the GTCSs by less than 3%. While even longer propagation times, and hence more expensive calculations, would be desirable, this suggests that we have effectively reached the long-time limit, in which the above procedure is rigorously valid.

Apparently, the resonance structure observed in the parallel geometry near 30 eV, at the equilibrium internuclear distance of $1.4 a_0$, cannot be attributed to different field-free propagation times. Moving to the perpendicular geometry, the two lowest doubly excited states of the ${}^1\Pi_u$ symmetry (again for $1.4 a_0$) are located, respectively, about 33.1 and 33.8 eV [21] above the ground state. By properly choosing the photon energy, these states are, in principle, accessible through single-photon absorption if the electric field has a component normal to the molecular axis. These autoionizing states lie, however, very close to the threshold for sequential DI and, most importantly, their energy widths are extremely narrow. For instance, the width of the lowest doubly excited ${}^1\Pi_u$ state is only about $8 \times 10^{-3} \text{ eV}$ [21], corresponding to a long lifetime of 82 fs. The pulse durations set in the present work, combined with the way we extract the results, would not allow us to resolve possible resonance effects related to these autoionizing states on the GTCSs for two-photon DI. Furthermore, the sharp rise of the cross section in the vicinity of 33-eV photon energy would make it very difficult to isolate the effects of the doubly excited states.

Figure 1(b) shows a comparison of the results obtained in the perpendicular and parallel geometries. In Ref. [11], the total cross section obtained with the simple model was shown up to a photon energy of 32.6 eV. Here we extend those results to 34.8 eV, i.e., just below the threshold for sequential DI. For the parallel case, the resonance structure around 30 eV was discussed in detail by Guan *et al.* [8]. Here we only note that the GTCS is overall about an order of magnitude larger in the perpendicular compared to the parallel geometry, thus indicating a very strong alignment effect. The simple model of Simonsen *et al.* [11] yields very reasonable results for both cases, except that it cannot reproduce the resonance effect. A further difference compared to the time-dependent calculations is the rapid rise of the cross section with photon energy as one approaches the threshold for sequential DI. Effects due to the energy resolution of the finite length pulses in *ab initio* solutions of the TDSE have been seen before and are most likely also the cause for the different slopes observed here. Nevertheless, when the photon energy approaches the threshold of sequential ionization, the sharp increase in the cross section is a general feature, which is independent of the relative orientation of the molecular axis and the laser polarization vector. The absolute values of the cross section, however, may differ significantly if this orientation is changed.

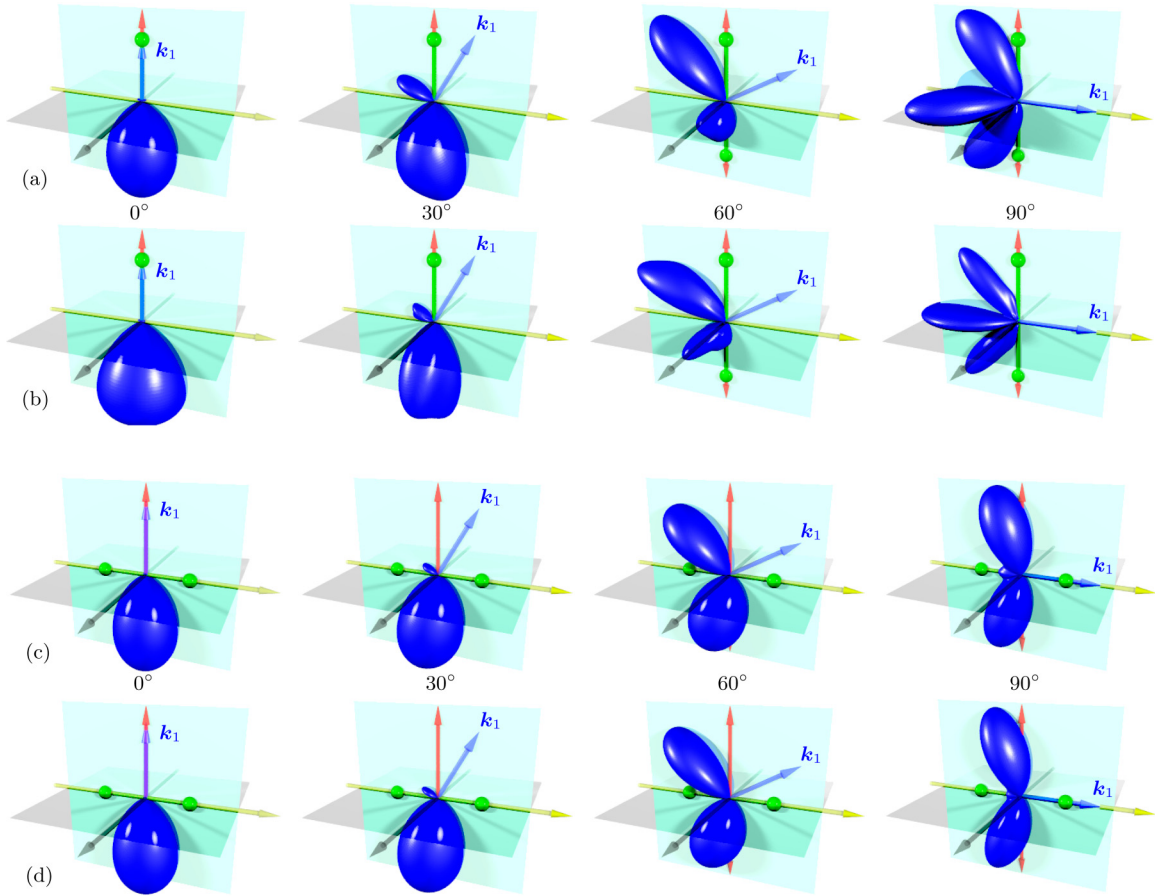


FIG. 2. (Color online) Angular distributions of the electrons ejected from the H_2 molecule at equal energy sharing ($E_1 = E_2 = 4.3$ eV) for the central photon energy of 30.0 eV in the FNA at the equilibrium distance of $1.4 a_0$. The laser polarization axis is represented by a double-headed arrow. (a) 10-cycle pulse in the parallel geometry. (b) 40-cycle pulse in the parallel geometry. (c) 10-cycle pulse in the perpendicular geometry. (d) 30-cycle pulse in the perpendicular geometry. One electron (k_1) is observed, respectively, at fixed angles (θ_1) of 0° , 30° , 60° , and 90° with respect to the laser polarization axis. Each panel has been individually scaled.

In Fig. 2, we display the angular distribution for a photon energy of 30.0 eV. For equal-energy sharing, when the fixed electron is observed along the molecular axis, the two electrons are predominantly ejected back to back. Comparing the predictions for the parallel geometry in rows (a,b) and the perpendicular geometry in rows (c,d), we see strong similarities in the two cases, especially when one of the electrons is observed along ($\theta_1 = 0^\circ$, first column) or near ($\theta_1 = 30^\circ$, second column) the laser polarization axis. Consequently, alignment effects manifest themselves in the magnitude (each panel is individually scaled, see below) but not so much in the shape of the angular distribution. Both alignment and pulse-length effects are clearly visible for $\theta_1 = 60^\circ$ (third column) and $\theta_1 = 90^\circ$ (fourth column). We will see, however, that the magnitude of the angular distributions drops rapidly when increasing θ_1 from 0° toward 90° . This is another example of the common experience that predictions for small cross sections are more sensitive to details in the physics and the numerical model than those for relatively large cross sections.

Figures 3 and 4 show the corresponding results for the perpendicular case only, but for incident energies of 26.5 and

34.0 eV, respectively. We note that pulse-length effects are only significant for large values of θ_1 , where the magnitudes of the angular distributions are again relatively small. The energy dependence in the shape of the angular distribution is also weak, once again mostly visible at $\theta_1 = 60^\circ$ and 90° .

The GTDCS in the coplanar geometry, where the internuclear axis, the laser polarization vector, and the linear momenta of the two ejected electrons all lie in the same plane, is shown in Figs. 5 (parallel case) and 6 (perpendicular case) for the central photon energy of 30.0 eV and symmetric energy sharing. For a number of detection angles θ_1 of one electron, measured relative to the direction of the linear laser polarization, the detection angle θ_2 of the other electron is varied. Our results are again compared with earlier predictions by Colgan *et al.* [9] and Morales *et al.* [10].

For the parallel case (Fig. 5), we note qualitative agreement in the angular dependence of the GTDCS predicted by the various methods, except perhaps for the overall smallest values occurring at $\theta_1 = 90^\circ$. Another exception is the increase in the TDCC results in the region where the two active electrons are traveling in about the same direction. This seems improbable for equal sharing of the excess energy and is

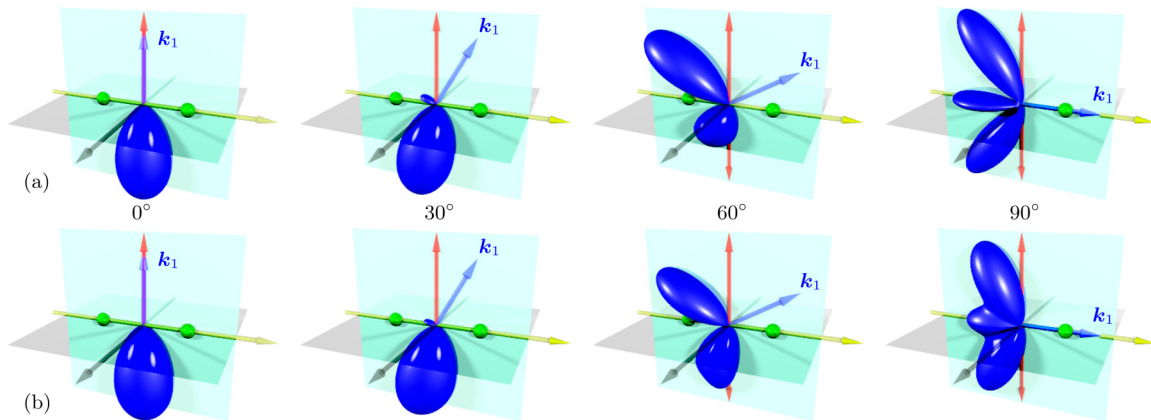


FIG. 3. (Color online) Angular distributions of the electrons ejected from the H_2 molecule at equal energy sharing ($E_1 = E_2 = 2.5$ eV) for the central photon energy of 26.5 eV in the FNA at the equilibrium distance of $1.4 a_0$. (a) 10-cycle pulse in the perpendicular geometry. (b) 30-cycle pulse in the perpendicular geometry.

most likely a numerical artifact in the early calculation [22]. We also see a significant effect of the pulse length, with the 40-cycle pulse producing larger values near the maxima of the angular distribution. This may, at least qualitatively, explain the differences between our results and those from the ECS calculation, which was effectively performed with an infinitely long pulse, i.e., no width in the frequency distribution.

For the perpendicular case (Fig. 6), on the other hand, the agreement with the TDCC predictions [9] is quite satisfactory, whereas serious discrepancies, again mostly in the magnitude, are seen with the ECS results [10]. Given the very small dependence on the pulse length for this case, it seems highly unlikely that these differences can be explained by the fixed frequency used in the ECS model.

Comparing the results for various values of θ_1 , we note a strong dependence of the predicted GTDCS on this angle. For the parallel case (Fig. 5), this dependence is seen in both the angular dependence and the magnitude, with the latter decreasing by about a factor of 4 in the maxima of the GTDCS. These maxima are also shifted to different θ_2 and even split in a variety of ways. In contrast, the maximum near $\theta_2 = 180^\circ$

in the perpendicular case (Fig. 6) remains more or less at this angle, but its magnitude drops by nearly a factor of 50 when going from $\theta_1 = 0^\circ$ to 90° . For the larger values of θ_1 , a second maximum develops. The patterns discussed above, except for the magnitude change, can also be seen as a cut through the appropriate plane in Fig. 2.

The significant drop in the magnitude of the GTDCS for the perpendicular geometry, as well as the overall energy dependence, is further illustrated in Fig. 7 for 26.5 and 34.0 eV, respectively. Once again the smallest cross sections exhibit the most detailed features, while the dominant cross section ($\theta_1 = 0^\circ$) simply shows a peak around $\theta_2 = 180^\circ$. Again, these patterns in the angular distribution can also be seen in Figs. 3 and 4.

Even though the angle- and energy-integrated GTCS is much larger for 34.0 than for 26.5 eV (Fig. 1), we note that it is the other way around for the maximum in the coplanar GTDCS. This is a consequence of (i) the increased excess energy available for the higher photon energies and (ii) the 34.0-eV case being dominated by asymmetric sharing of the excess energy, while symmetric energy sharing prevails

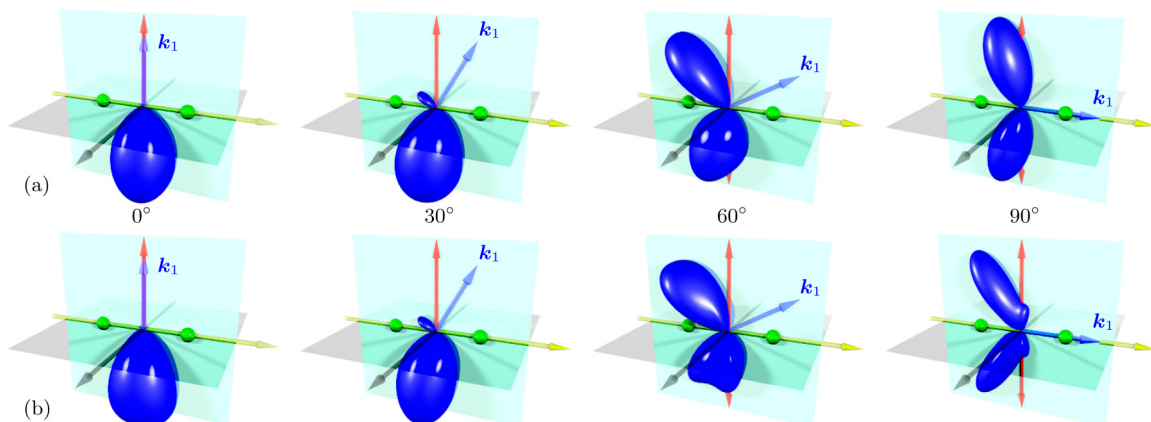


FIG. 4. (Color online) Angular distributions of the electrons ejected from the H_2 molecule at equal energy sharing ($E_1 = E_2 = 6.3$ eV) for the central photon energy of 34.0 eV in the FNA at the equilibrium distance of $1.4 a_0$. (a) 10-cycle pulse in the perpendicular geometry. (b) 30-cycle pulse in the perpendicular geometry.

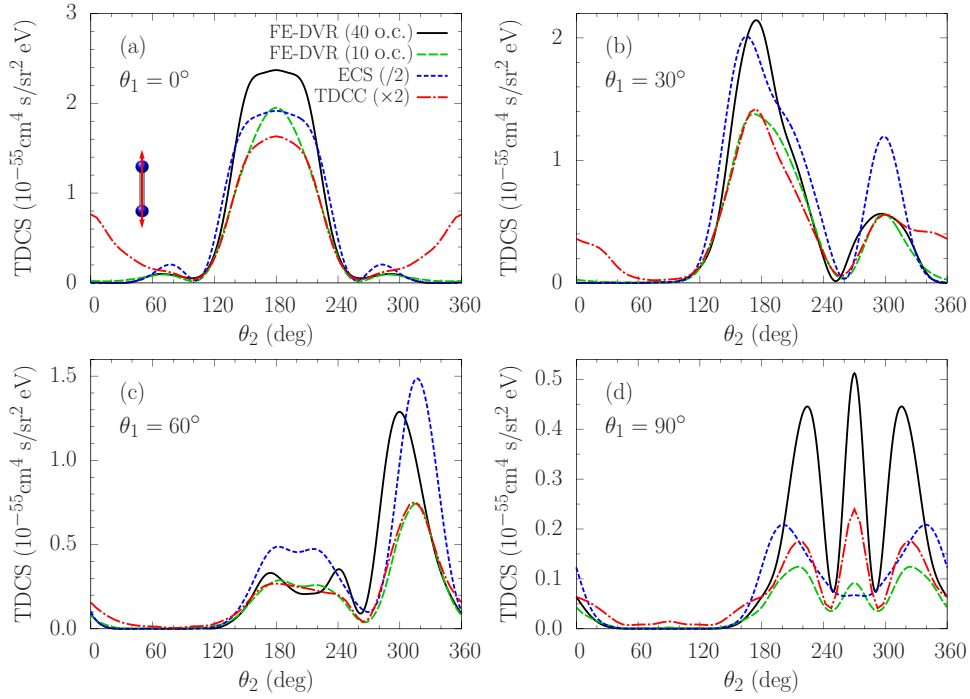


FIG. 5. (Color online) GTDCS in the coplanar geometry for electrons ejected from the H₂ molecule at equal energy sharing ($E_1 = E_2 = 4.3$ eV) in the parallel case for the central photon energy of 30.0 eV. The detection angle θ_1 of one electron is held fixed at 0° (a), 30° (b), 60° (c), or 90° (d), while the detection angle θ_2 is varied. The results from the present calculation for 10 and 40 o.c. are compared with predictions from earlier TDCC [9] and ECS [10] calculations. Note the scale factors in the legend of panel (a), which apply to all panels of this figure.

at the lower excess energies. Figures 6 and 7 show that the magnitude of the GTDCS in the dominant emission mode ($\theta_1 = 0^\circ$) at equal energy sharing decreases with increasing photon energy.

The latter dependence on the sharing of the excess energy is demonstrated in Fig. 8, where we chose a polar-plot representation of the results for the coplanar geometry. For 30 eV (see the panels in the left column of Fig. 8), we

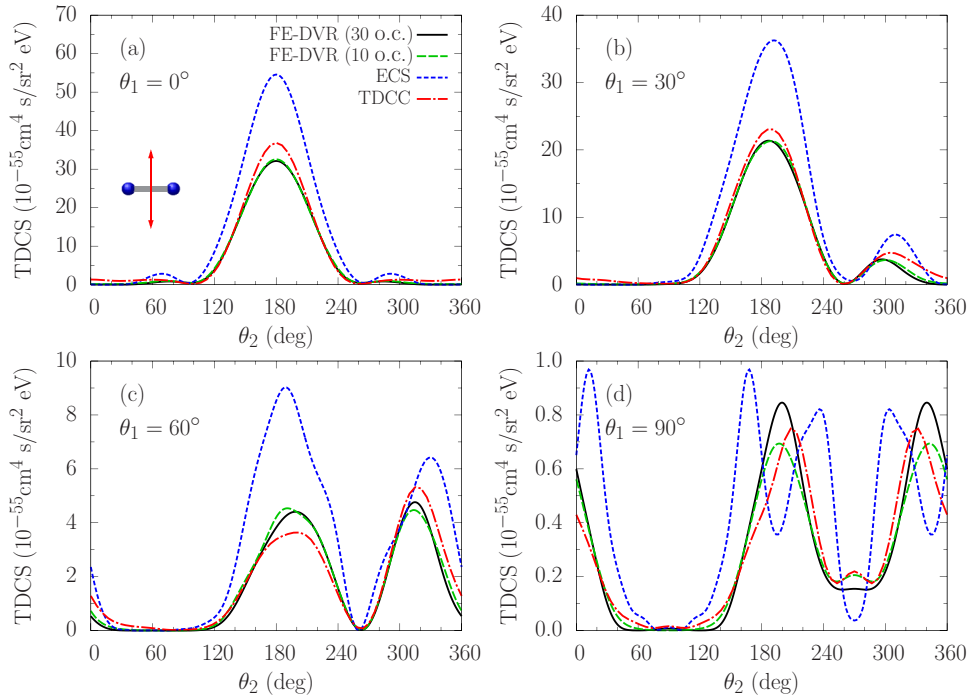


FIG. 6. (Color online) GTDCS in the coplanar geometry for electrons ejected from the H₂ molecule at equal energy sharing ($E_1 = E_2 = 4.3$ eV) in the perpendicular case for the central photon energy of 30.0 eV. The results from the present calculation for 10 and 30 o.c. are compared with predictions from earlier TDCC [9] and ECS [10] calculations. No scale factors were applied here.

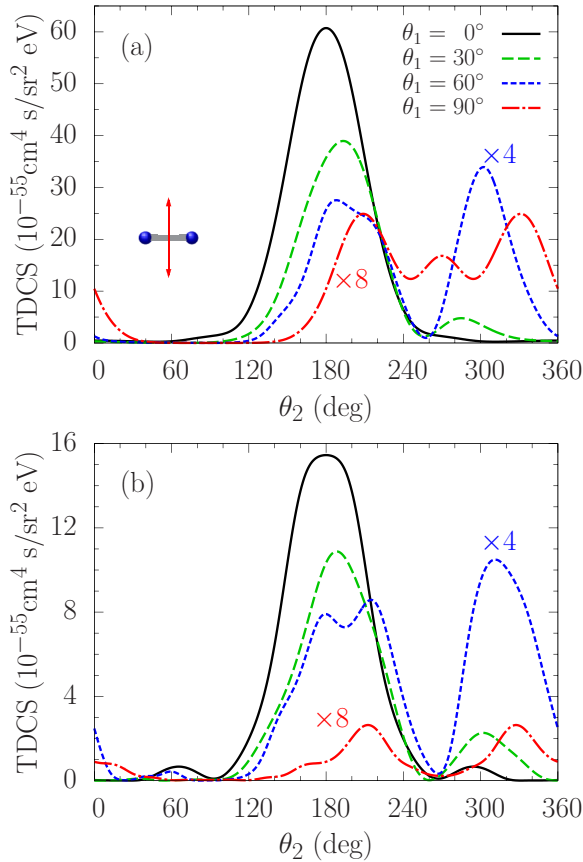


FIG. 7. (Color online) Same as Fig. 6 for central photon energies of 26.5 eV (a) and 34.0 eV (b), respectively. The results are from the present calculation for 30 o.c. No TDCS or ECS results are available for these cases. Note the scale factors for $\theta_1 = 60^\circ$ and 90° .

only notice a minor dependence of the GTDCS predictions on the relative fraction of sharing the excess energy, with the symmetric (50%:50%) case overall representing the least likely scenario. Once again, the largest effects due to varying the relative portions of the excess energy are seen for $\theta_1 = 90^\circ$. The GTDCS for this case, however, is very small compared to that for the dominant emission mode along the direction of the laser polarization. We note that Ivanov and Kheifets [23] also considered a case of unequal energy sharing, $E_1 : E_2 = 63% : 37%$, for the photon energy of 30 eV in the perpendicular geometry. They did not notice significant changes in the GTDCSs either, in agreement with our observation here.

As suggested above, asymmetric energy sharing becomes increasingly important when the threshold for sequential double ionization is approached. This is exhibited in the panels in the right column of Fig. 8. Also, the scale factors show that the drop in the magnitude of the GTDCS when going from $\theta_1 = 0^\circ$ to 90° is more pronounced for 34.0 than for 30.0 eV. While the patterns look most interesting for the larger values of θ_1 and could be used to test theoretical predictions most thoroughly, it seems unlikely that they would be experimentally observable—independent of the validity (or lack thereof) of the fixed-nuclei approximation.

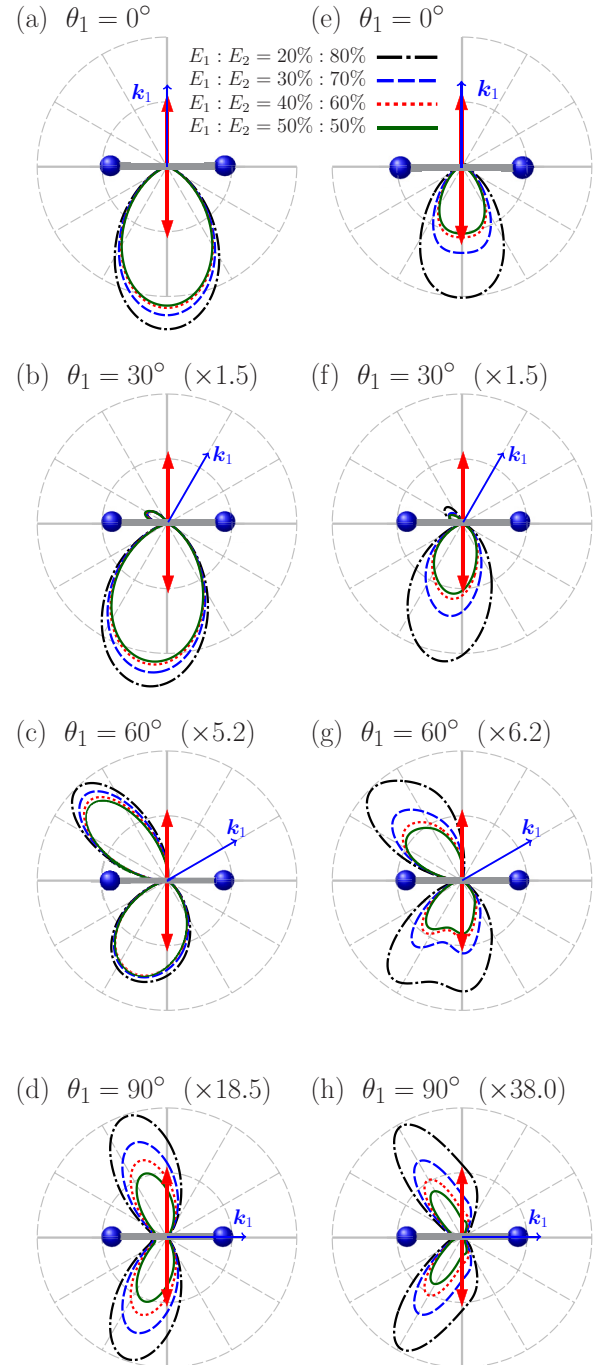


FIG. 8. (Color online) Coplanar GTDCS for central photon energies of 30.0 eV [left column, panels (a)–(d)] and 34.0 eV [right column, panels (e)–(h)]. The results are from the present calculation for 30 o.c. in the perpendicular case, for fixed angles $\theta_1 = 0^\circ, 30^\circ, 60^\circ,$ and 90° for different portions of the excess energy shared between the two outgoing electrons. The radius of the outer circle corresponds to $3 \times 10^{-54} \text{ cm}^4 \text{ s} / (\text{sr}^2 \text{ eV})$. Note the scale factors in the panels for $\theta_1 \neq 0^\circ$.

IV. CONCLUSIONS AND OUTLOOK

We have extended our previous investigation of alignment effects [5], this time in combination with a potential influence of the pulse length, on theoretical predictions for the

two-photon DI of H_2 at the level of the fixed-nuclei approximation. Due to the different symmetry of the one-photon intermediate state in the parallel and perpendicular geometries, resonance and pulse-length effects, which were clearly identified in the former case [8], are virtually nonexistent for a photon energy near 30 eV when the linear laser polarization vector and the internuclear axis are perpendicular to each other. The discrepancies between our results, those of Colgan *et al.* [9], and those of Morales *et al.* [10] could thus not be resolved in this case. Given the very challenging nature of the present problem, however, it is satisfying to see that our calculations support the results presented in the most recent work by Simonsen *et al.* [11], which was performed using an entirely independent method, but with very similar laser parameters.

In order to provide a more extensive dataset than is currently available in the literature, we presented detailed energy- and angle-resolved results for three different energies, chosen to be (i) close to the nonsequential double-ionization threshold as well as (ii) about halfway toward it, and finally (iii) close to the sequential double-ionization threshold. Furthermore, we showed results obtained for asymmetric energy sharing, which is the dominant mode for photon energies approaching the sequential DI threshold. This pattern in the energy distribution is also the reason for the sharp rise of the GTCSs in this energy regime. The present work in the perpendicular geometry hence complements and further supports our earlier conclusions, then drawn for the parallel case [8], regarding the general energy dependence of the GTCS near the threshold for sequential DI.

Our results are available in electronic form upon request. In the future, we hope to relax the restrictions in the FNA and account for the nuclear motion at least in some approximate way. With presently available computational resources, however, this is not a short-term project. In the meantime, it would be highly desirable to investigate the sources of the remaining discrepancies among the predictions of various theoretical groups by jointly studying a number of well-defined cases with exactly the same laser parameters and exactly the same kinematics, for both symmetric and asymmetric energy sharing as well as in-plane and out-of-plane geometries. The parameters used in the present calculation and in Simonsen *et al.* [11] seem highly appropriate for such a project. For the time-dependent calculations, we suggest a peak intensity of 10^{13} W/cm² and a \sin^2 envelope for the electric field. In this case, the effective interaction time is $35 \tau/128$ for a total pulse duration (see our definition at the end of Sec. II) of τ [3].

ACKNOWLEDGMENTS

We thank Dr. J. Colgan, Dr. M. Førre, and Dr. F. Morales for sending results in electronic form. This work was supported by the US NSF under Grants No. PHY-1068140 and No. PHY-1430245 (X.G. and K.B.); by super-computer resources on Kraken at Oak Ridge National Laboratory, Stampede, at the Texas Advanced Computer Center; and by super-computer resources on Gordon at the San Diego Supercomputing Center through the eXtreme Science and Engineering Discovery Environment (XSEDE) Allocation No. PHY-090031.

-
- [1] B. Bergues, M. Kübel, N. G. Johnson, B. Fischer, N. Camus, K. J. Betsch, O. Herrwerth, A. Senftleben, A. M. Sayler, T. Rathje, T. Pfeifer, I. Ben-Itzhak, R. R. Jones, G. G. Paulus, F. Krausz, R. Moshhammer, J. Ullrich, and M. F. Kling, *Nat. Commun.* **3**, 813 (2012).
- [2] X. Guan, O. Zatsarinny, C. J. Noble, K. Bartschat, and B. I. Schneider, *J. Phys. B* **42**, 134015 (2009).
- [3] X. Guan, K. Bartschat, and B. I. Schneider, *Phys. Rev. A* **77**, 043421 (2008).
- [4] H. Sann, T. Jahnke, T. Havermeier, K. Kreidi, C. Stuck, M. Meckel, M. S. Schöffler, N. Neumann, R. Wallauer, S. Voss, A. Czasch, O. Jagutzki, Th. Weber, H. Schmidt-Böcking, S. Miyabe, D. J. Haxton, A. E. Orel, T. N. Rescigno, and R. Dörner, *Phys. Rev. Lett.* **106**, 133001 (2011).
- [5] X. Guan, K. Bartschat, and B. I. Schneider, *Phys. Rev. A* **83**, 043403 (2011).
- [6] X. Guan, K. Bartschat, and B. I. Schneider, *Phys. Rev. A* **82**, 041404(R) (2010).
- [7] L. Avaldi and G. Stefani, in *Fragmentation Processes: Topics in Atomic and Molecular Physics*, edited by C. T. Whelan (Cambridge University Press, Cambridge, 2012), Chap. 1.
- [8] X. Guan, K. Bartschat, B. I. Schneider, and L. Koesterke, *Phys. Rev. A* **88**, 043402 (2013).
- [9] J. Colgan, M. S. Pindzola, and F. Robicheaux, *J. Phys. B* **41**, 121002 (2008).
- [10] F. Morales, F. Martín, D. A. Horner, T. N. Rescigno, and C. W. McCurdy, *J. Phys. B* **42**, 134013 (2009); the total cross section was not published in this paper, but was obtained via private communication from Dr. Morales.
- [11] A. S. Simonsen, S. A. Sørngård, R. Nepstad, and M. Førre, *Phys. Rev. A* **85**, 063404 (2012).
- [12] X. Guan, K. Bartschat, and B. I. Schneider, *Phys. Rev. A* **84**, 033403 (2011).
- [13] T. J. Park and J. C. Light, *J. Chem. Phys.* **85**, 5870 (1986).
- [14] F. H. M. Faisal, in *Theory of Multiphoton Processes* (Plenum, New York, 1987), Chap. 5.
- [15] J. Morelle, D. Normand, G. Mainfray, and C. Manus, *Phys. Rev. Lett.* **44**, 1394 (1980).
- [16] D. Charalambidis, D. Xenakis, C. J. G. J. Uiterwaal, P. Maragakis, J. Zhang, H. Schröder, O. Faucher, and P. Lambropoulos, *J. Phys. B* **30**, 1467 (1997).
- [17] C. J. Joachain, N. J. Kylstra, and R. M. Potvliege, in *Atoms in Intense Laser Fields* (Cambridge University Press, Cambridge, 2012), Chap. 3.
- [18] X. Guan, R. C. DuToit, and K. Bartschat, *Phys. Rev. A* **87**, 053410 (2013).
- [19] L. B. Madsen, L. A. A. Nikolopoulos, T. K. Kjeldsen, and J. Fernández, *Phys. Rev. A* **76**, 063407 (2007).
- [20] J. Feist, S. Nagele, R. Pazourek, E. Persson, B. I. Schneider, L. A. Collins, and J. Burgdörfer, *Phys. Rev. A* **77**, 043420 (2008).
- [21] I. Sánchez and F. Martín, *J. Chem. Phys.* **106**, 7720 (1997).
- [22] J. Colgan (private communication).
- [23] I. A. Ivanov and A. S. Kheifets, *Phys. Rev. A* **87**, 023414 (2013).